

文章编号:1006-9941(2020)03-0190-08

## Synthesis and Third-order Nonlinear Optical Properties of *N*-(6-hexanol)-2-methoxy-8-nitroazophenyl Carbazole

ZHONG Quan-jie<sup>1,2</sup>, ZHENG Jian<sup>2</sup>, ZHANG Lin<sup>1</sup>, LUO Xuan<sup>1</sup>

(1. Research Center of Laser Fusion, China Academy of Engineering Physics, Mianyang 621999, China; 2. University of Science and Technology of China, Hefei 230026, China)

**Abstract:** A new compound *N*-(6-hexanol)-2-methoxy-8-nitroazophenyl carbazole (HMNAC) was synthesized by electrophilic substitution reaction and post-azo-coupling reaction, and the structure of HMNAC was characterized by IR, <sup>1</sup>H NMR and <sup>13</sup>C NMR. The molecular structure of HMNAC was optimized at the B3LYP/6-31G(d) level. Single point energy was calculated at the MP2/6-31G(d) level. The relative energy  $E_r$  between *cis-trans* isomers of HMNAC was found to be 52.43 kJ·mol<sup>-1</sup>. The third-order nonlinear optical properties of HMNAC were studied by Z-scan technique under nanosecond excitation at 532 nm. Closed-aperture curve has revealed that HMNAC has self-defocusing effect. Open-aperture curve indicated that both saturated absorption and reverse saturated absorption exist in HMNAC. The second-order hyperpolarizability  $\gamma$  of HMNAC was 2.59×10<sup>-29</sup> esu, and the figure of merits (FOMs) reached 1.5.

**Key words:** *N*-(6-hexanol)-2-methoxy-8-nitroazophenyl carbazole (HMNAC); density functional theory; *cis-trans* isomers; Z-scan; third-order nonlinear optical properties

CLC number: TJ55;O649

Document code: A

DOI: 10.11943/CJEM2019101

### 1 Introduction

The synthesis and development of new energetic materials continue focusing on the nitrogen-containing heterocyclic compounds with high density, high heat of formation and low sensitivity<sup>[1-2]</sup>. In order to ensure the safety of energetic materials in storage and transportation, these materials must have low sensitivity<sup>[1-2]</sup>. Azo compounds have both *cis*-isomer and *trans*-isomer, usually in the form of *trans*-isomer<sup>[3]</sup>. Under the action of light and heat, azo compounds have the characteristics of reversible *cis-trans* isomerization<sup>[3]</sup>. Upon external stimulation, the

rapid conversion of the *trans*- to the *cis*-configuration converts the excitation energy into the internal energy of the *cis*-configuration, and reduces the energy obtained in the subsequent recovery from *cis-trans* configuration, which to some extent avoids the decomposition of such energetic compounds<sup>[4]</sup>. Therefore, azo energetic compounds can generate self-desensitization effect by means of the *cis-trans* isomerization process<sup>[4]</sup>. Using the self-desensitization effect of azo energetic compounds, high safety explosives and rocket propellants can be designed<sup>[4]</sup>. In addition, many nonlinear optical materials can be prepared by using the *cis-trans* conversion of azo compounds under light conditions<sup>[3]</sup>. Azo nonlinear optical materials have attracted many interests because of their potential applications in all-optical signal processing, optoelectronic devices, all-optical switching, optical image processing, optical information storage, optical limiting, optical waveguides and high speed optical communication networks<sup>[5-9]</sup>. In

Received Date: 2019-04-16; Revised Date: 2019-07-21

Published Online: 2019-10-14

**Biography:** ZHONG Quan-jie (1991-), male, PhD, research field: the synthesis of nonlinear optical materials.

e-mail: quanjiezhong@163.com

**Corresponding author:** LUO Xuan (1976-), male, associate research fellow, research field: the synthesis of target materials.

e-mail: luox76@gmail.com

引用本文: 钟全洁, 郑坚, 张林, 等. *N*-(6-羟基己基)-2-甲氧基-8-硝基苯偶氮基咔唑的合成与三阶非线性光学性能[J]. 含能材料, 2020, 28(3):190-197.

ZHONG Quan-jie, ZHENG Jian, ZHANG Lin, et al. Synthesis and Third-order Nonlinear Optical Properties of *N*-(6-hexanol)-2-methoxy-8-nitroazophenyl Carbazole[J]. *Chinese Journal of Energetic Materials (Hanneng Cailiao)*, 2020, 28(3):190-197.

the past few decades, organic materials have been intensively investigated since they exhibit large third-order nonlinear optical susceptibilities  $\chi^{(3)}$  compared to the traditional inorganic nonlinear optical materials such as barium metaborate, Lithium triborate and lithium niobate crystal<sup>[10-12]</sup>. In particular, organic nonlinear optical materials can be designed at the molecular level in order to achieve the best nonlinear optical properties<sup>[12]</sup>. The study of the excellent third-order nonlinear optical materials and new structure are a very challenging task<sup>[13-14]</sup>. The relationship between the molecular structure and nonlinear optical properties has been studied deeply<sup>[15]</sup>.

Previous research had discovered that the  $\pi$ -conjugated system was more efficient than other electron structure in exhibiting nonlinear optical effects<sup>[16-18]</sup>. Electron donor and electron acceptor could also enhance nonlinear optical effects<sup>[13-14, 16]</sup>. Thus, molecule units containing highly delocalized  $\pi$ -conjugated system and strong electron acceptor and electron donor would lead to larger second-order hyperpolarizabilities  $\gamma$ . A series of compounds containing identical  $\pi$ -bridge and electron-donating groups, but with different electron-withdrawing groups were recently reported<sup>[19]</sup>. Research showed that the third-order nonlinear optical properties were enhanced by increasing electron-withdrawing ability<sup>[19]</sup>. The third-order nonlinear optical susceptibilities  $\chi^{(3)}$  and the second-order hyperpolarizabilities  $\gamma$  can reach up to  $6.03 \times 10^{-13}$  esu,  $2.01 \times 10^{-31}$  esu, respectively<sup>[19]</sup>. Based on our own previous works, *N*-6-hydroxy-hexyl-4-azophenyl-carbazole was synthesized and studied. Theoretical calculations and experimental results showed that *N*-6-hydroxy-hexyl-4-azophenyl-carbazole was an excellent third-order nonlinear optical material, and its third-order nonlinear optical effects derived from the charge-transfer excitation and the local excitation where the charge-transfer excitation plays a leading role<sup>[20]</sup>. Moser et al. pointed out that the design and development of organic nonlinear optical materials should use intramolecular electron transfer to form the charge transfer state<sup>[21]</sup>. In the family of organic nonlinear optical materials,

azobenzene and carbazole have received much attention<sup>[22]</sup>. Azobenzene and carbazole contain larger  $\pi$ -conjugated electronic systems and stronger intramolecular electron transfer<sup>[23]</sup>. The electron-rich structure makes it easy to introduce various functional groups in the electrophilic substitution reaction to adjust the nonlinear optical properties<sup>[24-25]</sup>. However, in order to meet the actual needs for low-power photonics applications, the nonlinear optical effects and FOMs of organic materials needed to be further improved.

In this article, we reported HMNAC prepared via electrophilic substitution reaction and post-azocoupling reaction. The relative energy  $E_r$  between the *trans*-isomer and *cis*-isomer was calculated at the MP2/6-31G(d)//B3LYP/6-31G(d) level. The standard Z-scan technique was utilized to investigate the third-order nonlinear optical properties of HMNAC. Further, the nonlinear optical effects and FOMs were calculated and analyzed.

## 2 Experiments

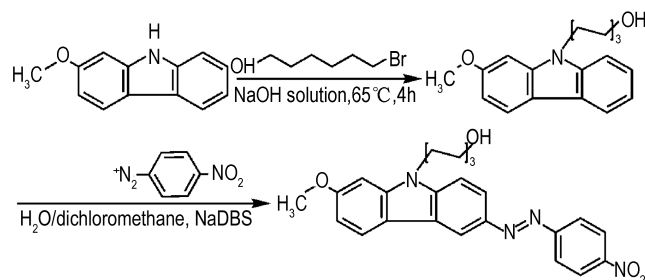
### 2.1 Materials and Measurements

2-Methoxycarbazole and 6-bromo-1-hexanol were purchased from Tokyo Chemical Industry. Dimethyl sulfoxide (DMSO), benzyl triethyl ammonium chloride, sodium hydroxide, ethyl acetate, anhydrous sodium sulfate, dichloromethane, 4-Nitroaniline, hydrochloric acid, sodium nitrite, sodium dodecyl benzenesulfonate and petroleum ether were obtained from Chengdu Chron Chemicals. Dimethyl sulfoxide was chromatographical grade. All chemicals used without further purification. Heating stirrer was an IKA magnetic heating stirrer. Infrared spectra were obtained from KBr pellet on a PerkinElmer Spectrum One infrared spectrometer in the range of 4000–400  $\text{cm}^{-1}$ .  $^1\text{H}$  NMR and  $^{13}\text{C}$  NMR were obtained in  $\text{DMSO}-d_6$  on a Bruker AV600 NMR spectrometer.

### 2.2 Synthesis and Characterization

*N*-(6-hexanol)-2-methoxy carbazole was firstly prepared via electrophilic substitution reaction from

2-methoxy carbazole. Then, HMNAC was prepared through post-azo-coupling reaction from *N*-(6-hexanol)-2-methoxy carbazole. The synthetic route of HMNAC is summarized in Scheme 1.



**Scheme 1** Synthetic route of HMNAC

### 2.2.1 Synthesis of *N*-(6-hexanol)-2-methoxy Carbazole

2-methoxy carbazole (1.97 g, 10 mmol), 6-bromo-1-hexanol (1.57 mL, 12 mmol) and benzyl triethyl ammonium chloride (150 mg) were dissolved in DMSO (40 mL). To the stirred solution, sodium hydroxide (2.0 g, 50 mmol), as a concentrated aqueous solution, was added and magnetic stirring was continued for 4 h at 65 °C. After the reaction, the mixture was cooled to room temperature. The mixture was extracted with ethyl acetate (50 mL). The combined organic layer was then washed with water, dried over anhydrous sodium sulfate, filtered, and concentrated under reduced pressure. The residue was purified by silica gel column chromatography (eluent, dichloromethane) to afford 2.67 g (9 mmol, 90%) of the target compound *N*-(6-hexanol)-2-methoxy carbazole. IR (KBr,  $\nu/\text{cm}^{-1}$ ) 3389, 3049, 2996, 2932, 2857, 1630, 1601, 1499, 1464, 1246, 1200, 1169, 815, 746;  $^1\text{H}$  NMR (600 MHz, DMSO- $d_6$ )  $\delta$ : 8.01 (d,  $J=7.8$  Hz, 1H), 7.99 (d,  $J=8.4$  Hz, 1H), 7.50 (d,  $J=8.4$  Hz, 1H), 7.35 (t,  $J=7.8$  Hz, 1H), 7.14 (t,  $J=7.8$  Hz, 1H), 7.09 (d,  $J=1.8$  Hz, 1H), 6.80 (dd,  $J=2.4$  Hz, 9.0 Hz, 1H), 4.38 (t,  $J=5.4$  Hz, 1H), 4.33 (t,  $J=7.2$  Hz, 2H), 3.88 (s, 3H), 3.33 (q,  $J=6.0$  Hz, 2H), 1.75 (m, 2H), 1.30 (m, 4H), 1.30 (m, 4H);  $^{13}\text{C}$  NMR (150 MHz, DMSO- $d_6$ )  $\delta$ : 158.97, 141.73, 140.54, 124.31, 122.98, 121.02, 119.45, 118.85, 116.80, 108.38, 106.86, 93.28, 62.62, 55.68, 42.83, 32.48,

28.74, 26.99, 25.49.

### 2.2.2 Synthesis of HMNAC

4-Nitroaniline (1.12 g, 8 mmol) was dissolved in a solution of concentrated hydrochloric acid (5 mL) in water (80 mL). The mixture was cooled in an ice bath until the temperature was below 5 °C. Then a solution containing sodium nitrite (0.66 g, 9.6 mmol) in water (3 mL) was added slowly to the 4-nitroaniline solution. The mixture was allowed to magnetic stirring in the ice bath for 30 min. While the mixture was still kept in the ice bath, sodium dodecyl benzenesulfonate (0.2 g) was added. A solution of *N*-(6-hexanol)-2-methoxy carbazole (2.38 g, 8 mmol) in dichloromethane (60 mL) was added to the above mixture. The resultant mixture was stirred vigorously at room temperature for 24 h. After the reaction, the mixture was concentrated under reduced pressure, filtered. The residue was purified by silica gel column chromatography (eluent, petroleum ether/ethyl acetate=1:1) to afford 1.78 g (4 mmol, 50%) of the target compound HMNAC. IR (KBr,  $\nu/\text{cm}^{-1}$ ) 3412, 3049, 2935, 2859, 1630, 1599, 1519, 1461, 1334, 1235, 1134, 860, 744;  $^1\text{H}$  NMR (600 MHz, DMSO- $d_6$ )  $\delta$ : 8.50 (s, 1H), 8.44 (t,  $J=2.4$  Hz, 1H), 8.43 (t,  $J=1.8$  Hz, 1H), 8.17 (d,  $J=7.8$  Hz, 1H), 8.04 (t,  $J=1.8$  Hz, 1H), 8.03 (t,  $J=1.8$  Hz, 1H), 7.60 (d,  $J=8.4$  Hz, 1H), 7.44 (t,  $J=8.4$  Hz, 1H), 7.37 (s, 1H), 7.23 (t,  $J=7.8$  Hz, 1H), 4.44 (t,  $J=7.2$  Hz, 2H), 4.32 (t,  $J=5.4$  Hz, 1H), 4.12 (s, 3H), 3.35 (t,  $J=5.4$  Hz, 2H), 1.82 (m, 2H), 1.36 (m, 4H), 1.23 (m, 2H);  $^{13}\text{C}$  NMR (150 MHz, DMSO- $d_6$ )  $\delta$ : 158.16, 156.14, 147.23, 145.02, 141.09, 136.25, 125.73, 124.97, 123.19, 122.86, 120.28, 120.04, 115.96, 109.76, 107.81, 92.82, 60.47, 56.49, 42.31, 32.35, 28.22, 26.18, 25.16.

### 2.3 Quantum Chemistry Calculation

Density functional theory and second-order Møller-Plesset perturbation theory have been utilized to study the self-desensitization effect of HMNAC. The geometric structure of *cis-trans* isomers of HMNAC was calculated at the B3LYP/6-31G(d) level. Harmonic vibrational frequencies were calculated to confirm the stable configurations and transition

states at the B3LYP/6-31G(d) level. Zero-point vibrational energy (*ZPE*) was obtained by frequency calculation. Single point energy calculation was carried out at the MP2/6-311G(d) level. All calculations are based on Gaussian 09 package.

#### 2.4 Third-order Nonlinear Optical Measurements

The third-order nonlinear optical properties were measured by Z-scan using the 4 ns laser pulses generated by the DAWA-S Pulse Q-switched Laser system with the repetition rate of 10 Hz and the wavelength of 532 nm. The experiments were performed in dichloromethane solutions using a 2 mm-thick quartz cuvette at room temperature. The concentration of HMNAC was  $6.67 \times 10^{-4} \text{ mol} \cdot \text{L}^{-1}$ . The laser beam was focused on the sample by a lens of focal length 250 nm. The radius of the beam waist  $\omega_0$  was calculated to be 19  $\mu\text{m}$ . The Rayleigh length  $z_0 = \pi\omega_0^2/\lambda$  was calculated to be 2.13 mm, which is greater than the thickness of the sample cuvette. The reference beam energy, probe beam energy were measured simultaneously using an energy ratio meter (Rj-7620). The distance between the detector and the focus of the lens was far enough to satisfy the far-field approximation. Before measuring this sample, the third-order nonlinear optical properties of a standard sample (ZnSe) were observed.

### 3 Results and Discussion

#### 3.1 Synthesis

*N*-(6-hexanol)-2-methoxy carbazole was obtained by via electrophilic substitution reaction from 2-methoxy carbazole. In order to improve the yield of target compound, it is necessary to control the mole ratio of 2-methoxy carbazole to 6-bromohexanol and reaction time. The optimum synthesis conditions were mole ratio of 2-methoxy carbazole to 6-bromohexanol 1:1.2, and the reaction time 4h. As for the synthesis of HMNAC, a post-functionalization method was selected. The benzene ring system is susceptible to electrophilic attack and couple with diazonium salts, but the carbazole system is not as easy as that on the benzene ring system<sup>[24]</sup>. For the

carbazole system, it was reported that the azo coupling could be made more efficient in a two-phase system in the presence of the phase transfer catalyst sodium dodecyl benzenesulfonate<sup>[26]</sup>. Dichloromethane and water were selected as the reaction medium in our work for its excellent solubility to the reactants. Both the bulkiness of the introduced functional group and steric effect of the azo coupling product would make the electrophilic substitution to take place exclusively at the 8-position of *N*-(6-hexanol)-2-methoxy carbazole. Target product HMNAC is red powder and easily soluble in common organic solvents like chloroform, dichloromethane, tetrahydrofuran and dimethyl sulfoxide.

#### 3.2 Molecular Structure and Relative Energy of *Trans-cis* Isomers

The optimized geometries of *trans*-HMNAC and *cis*-HMNAC were shown in Figure 1 and the atomic labels were marked out. There is no imaginary frequency in frequency calculation which indicated that we get the stability configuration of the local minimum in the potential energy surface.

In order to improve the energy accuracy, single

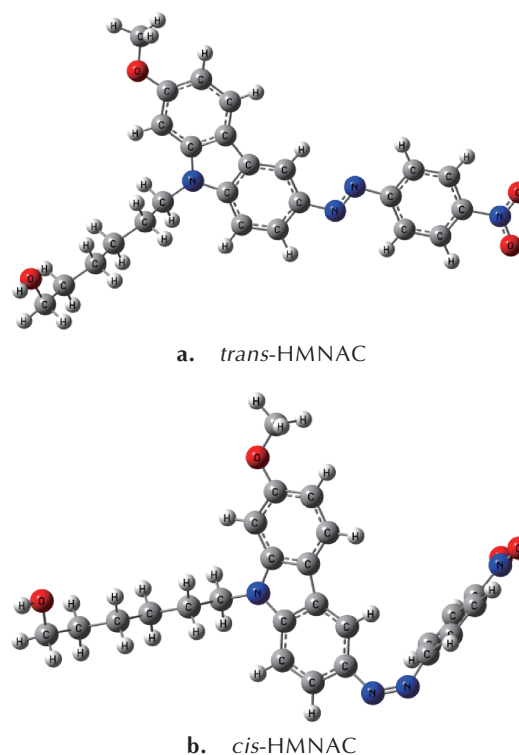


Fig. 1 Optimized molecular structures of HMNAC

point energy calculation was carried out at the MP2/6-31G(d) level. Relative energy  $E_r$  of *cis-trans* isomers was obtained after ZPE correction. Total energy ( $E$ ), zero-point vibrational energy (ZPE) and relative energy ( $E_r$ ) of *trans*-HMNAC and *cis*-HMNAC were shown in Table 1. Compared to *cis*-HMNAC, *trans*-HMNAC has a lower energy. Normally, HMNAC exists mainly in the form of *trans*-isomer. Upon external stimulation, the rapid conversion of *trans*- to *cis*-HMNAC converts the excitation energy into the internal energy of the *cis*-HMNAC which avoids the decomposition of such energetic compounds. Relative energy  $E_r$  between *trans*-HMNAC and *cis*-HMNAC reached  $52.43 \text{ kJ}\cdot\text{mol}^{-1}$ . HMNAC exhibits low sensitivity.

**Table 1** Total energy ( $E$ ), zero-point vibrational energy (ZPE) and relative energy ( $E_r$ ) of *trans*-HMNAC and *cis*-HMNAC

HMNAC	$E / \text{a.u.}$	ZPE / $\text{kJ}\cdot\text{mol}^{-1}$	$E_r / \text{kJ}\cdot\text{mol}^{-1}$
<i>trans</i>	-1483.5030226	1257.46	0.00
<i>cis</i>	-1483.4824737	1255.95	52.43

### 3.3 Optical Properties

The linear absorption spectrum is shown in Figure 2. HMNAC exhibited two strong bands in UV-Vis beyond 300 nm. The band at near-ultraviolet is owing to excitation from  $\pi \rightarrow \pi^*$  of the carbon-carbon bond, while the band at the visible spectral region is related to excitation from  $n \rightarrow \pi^*$  of the nitrogen-nitrogen bond.

### 3.4 Third-order Nonlinear Optical Properties

Z-scan measurements were performed at 532 nm as shown in Figure 3a and Figure 3b. Figure 3a and

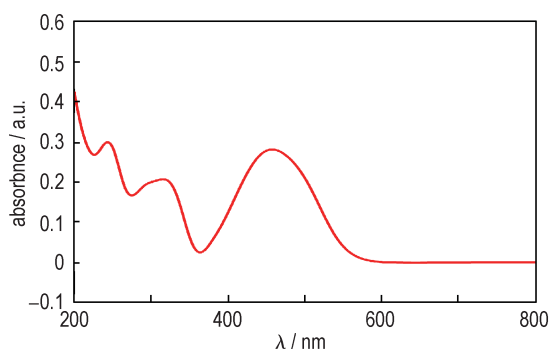


**Fig. 2** UV - visible absorption spectrum of HMNAC

Figure 3b exhibit the open-aperture and closed-aperture Z-scan curves, respectively.

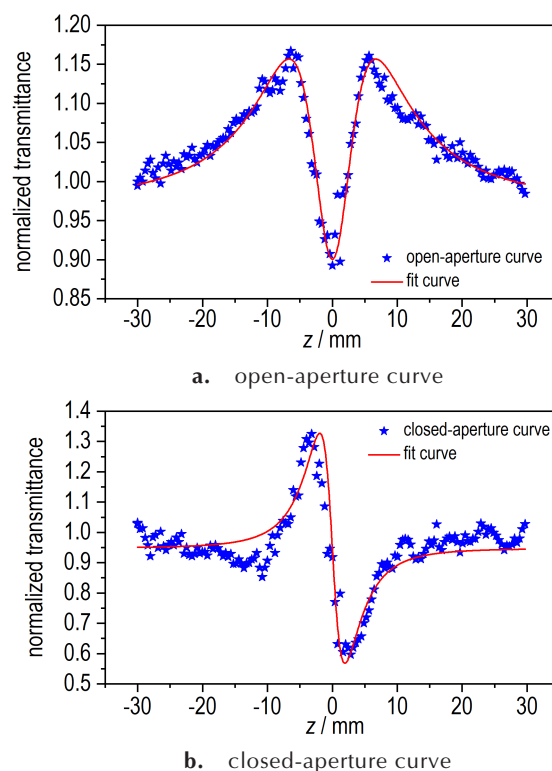


**Fig. 3** Z-scan curve of HMNAC

The irradiance at focus of the laser beam  $I_0$  was calculated as  $2.21 \times 10^{12} \text{ W}\cdot\text{m}^{-2}$ . The peak-to-valley configuration of the closed-aperture curve indicated that the refractive-index change is negative, exhibiting a self-defocusing effect<sup>[27]</sup>. The M-type curve indicated that both saturated absorption and reverse saturated absorption exist<sup>[28]</sup>. The saturated absorption is caused by the transition from ground state to excited state. The reverse saturated absorption is mainly caused by the transition between excited states.

The energy levels with different structures of organic molecules can be described by a five-level model including singlet and triplet states<sup>[29]</sup>. Figure 4 showed the five-level model of organic molecular system, in which  $S_0$  is the ground state;  $S_1$  and  $S_2$  are the first excited state and upper excited state in singlet, respectively;  $T_1$  and  $T_2$  are the first excited state and upper excited state in triplet, respectively; and every electronic energy level contains many vibra-

tional or rotational energy levels. When a beam of light with a frequency of  $\omega$  irradiates the molecular system, the photons would be absorbed by molecules in the ground state, which causes the transition of molecules from 0, to 1' with absorption cross section  $\sigma_0$ . The lifetime of energy level 1' is very short. It relaxes rapidly downward to lower energy level 1, and then to energy level 0 and 3 through non-radiative transition and intersystem crossing, respectively. At room temperature, the probability of stimulated radiation of organic molecules is very small and can be neglected. For organic molecules, the intersystem crossing time  $\tau_{ST}$  is less than  $\tau_1$  and nanoseconds, which is mainly because of the nanosecond regime of pulse duration in our measurement. Meanwhile, the intersystem crossing time  $\tau_T$  is longer than nanoseconds. The five-level model is simplified as an effective four-level system with  $S_0, S_1, T_1$  and  $T_2$  states. The saturated absorption is determined by the balance of the number of particles between triplet  $T_1$  and ground state  $S_0$  and the reverse saturated absorption is determined by the balance of the number of particles between triplet state  $T_2$  and triplet state  $T_1$ .

The nonlinear absorption coefficient  $\beta$  can be obtained from a best fitting performed on the experimental data of the open-aperture Z-scan with the equation<sup>[30]</sup>:

$$T(z) = \sum_0^{+\infty} \frac{[-\beta I_0 L_{\text{eff}} / (1 + z^2/z_0^2)]^m}{(m+1)^{3/2}} \quad (1)$$

Where  $I_0$  is the intensity of beam at focus,  $L_{\text{eff}} = (1 - \exp(-\alpha_0 L)) / \alpha_0$  is the effective length,  $\alpha_0$  is the linear absorption coefficient,  $L$  is the thickness of the sample,  $z$  the longitudinal displacement of the sample from the focus and  $z_0$  is the Rayleigh diffraction length.

To obtain the nonlinear refractive index  $n_2$ , we can fit the experiment data of the closed-aperture Z-scan with the equation<sup>[30]</sup>:

$$T(z) = 1 + \frac{4\Delta\Phi_0 x}{(x^2 + 9)(x^2 + 1)} \quad (2)$$

Where  $\Delta\Phi_0 = kn_2 I_0 L_{\text{eff}}$  is the on-axis nonlinear phase shift at the focus,  $k = 2\pi/\lambda$  is the wave vector,  $x = z/z_0$ .

The third-order optical nonlinear susceptibility

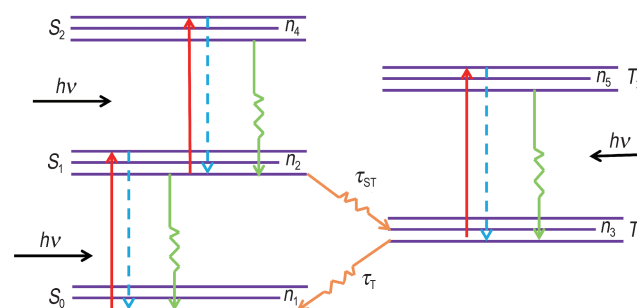


Fig. 4 The five-level model of organic molecular system

$\chi^{(3)}$  of materials can be written as<sup>[30]</sup>:

$$\chi^{(3)} = \text{Re}\chi^{(3)} + i\text{Im}\chi^{(3)} \quad (3)$$

$$\text{Re}\chi^{(3)}(\text{esu}) = \frac{cn_0^2}{120\pi^2} n_2 \quad (4)$$

$$\text{Im}\chi^{(3)}(\text{esu}) = \frac{c^2 n_0^2}{240\pi^2 \omega} \beta \quad (5)$$

Where  $n_0$  is the linear refractive index of the sample,  $\omega$  is the angular frequency of the light field and  $c$  is the velocity of light in vacuum.

The second-order hyperpolarizability  $\gamma$  of the molecules can be written as<sup>[19]</sup>:

$$\gamma = \chi^{(3)} / NL \quad (6)$$

Where  $N$  is the number of molecules of unit volume;  $L$  is the local field correction factor, which is defined as  $L = [n(\omega)^2 + 2]^4 / 81$ , where  $n(\omega)$  is the refractive index.

The obtained results are summarized in Table 2.

Table 2 Summary of nonlinear optical properties of HMNAC

$I_0 / \text{GW} \cdot \text{m}^{-2}$	$\beta / \text{m} \cdot \text{W}^{-1}$	$n_2 / \text{m}^2 \cdot \text{W}^{-1}$	$\chi^{(3)} / \text{esu}$	$\gamma / \text{esu}$
0.22	$8.17 \times 10^{-11}$	$-6.53 \times 10^{-17}$	$3.34 \times 10^{-11}$	$2.59 \times 10^{-29}$

The third-order optical nonlinear susceptibility  $\chi^{(3)}$  of HMNAC was calculated as  $3.34 \times 10^{-11}$  esu. The interaction of intramolecular valence bond is stronger than that of intermolecular Van der Waals forces, so coupling interaction is weak between electronic structure of the single molecule and the surrounding molecules. Each molecule can be regarded as an independent polarization source. The coupling of adjacent molecules is mainly realized by the local field. Therefore, we can establish the equivalence relation between micro and macro properties. The second-order hyperpolarizability  $\gamma$  of HMNAC was cal-

culated as  $2.59 \times 10^{-29}$  esu through equation (6). Compared with the second-order hyperpolarizability  $\gamma$  of carbon disulfide as a standard reference sample for nonlinear optical study, HMNAC exhibits excellent third-order nonlinear optical properties. In particular,  $FOMs$  is defined as  $FOMs = n_2 / \beta \lambda^{[31]}$ . With the date,  $n_2 = 6.53 \times 10^{-17} \text{ m}^2 \cdot \text{W}^{-1}$ ,  $\beta = 8.17 \times 10^{-11} \text{ m} \cdot \text{W}^{-1}$  and  $\lambda = 532 \text{ nm}$ ,  $FOMs$  was calculated to be 1.5, which is critical in all-optical switching device.

## 4 Conclusions

We have synthesized a new compound HMNAC and its structure was characterized by IR spectrum,  $^1\text{H}$  NMR spectrum and  $^{13}\text{C}$  NMR spectrum. The *trans-cis* isomerization was studied based on the density functional theory and the second-order Møller-Plesset perturbation theory. Relative energy  $E_R$  between *trans*-HMNAC and *cis*-HMNAC reached to  $52.43 \text{ kJ} \cdot \text{mol}^{-1}$ . HMNAC exhibits low sensitivity and is expected to be used in high safety explosives and rocket propellants. The third-order nonlinear optical properties of HMNAC were investigated using Z-scan technique. Second-order hyperpolarizability  $\gamma$  and  $FOMs$  are  $2.59 \times 10^{-29}$  esu and 1.5, respectively. HMNAC is a good candidate for the development of low-power, high-contrast all-optical switching device.

## References:

- [1] Thottempudi V, Forohor F, Parrish D A, et al. Tris (triazolo) benzene and Its Derivatives: High-Density Energetic Materials [J]. *Angewandte Chemie International Edition*, 2012, 51(39): 9881–9885.
- [2] Thottempudi V, Zhang J, He C, et al. Azo substituted 1, 2, 4-oxadiazoles as insensitive energetic materials [J]. *RSC Advances*, 2014, 4(92): 50361–50364.
- [3] ZHANG Lu-bo, ZHAO Xiu-xiu, PANG Si-ping, et al. Research progress on the synthesis of aromatic azo compounds [J]. *Chinese Journal of Synthetic Chemistry*, 2014, 22(5): 709–724.
- [4] Luoxin Wang, Xinlin Tuo, Changhai Yi, et al. Theoretical study on the *trans-cis* isomerization and initial decomposition of energetic azofurazan and azoxyfurazan [J]. *Journal of Molecular Graphics and Modelling*, 2009, 28(2): 81–87.
- [5] Joel M H, Jonathan M, Stephen B, et al. Design of polymethine dyes with large third-order optical nonlinearities and loss figures of merit [J]. *Science*, 2010, 327(5972): 1485–1488.
- [6] Hayk H, Giorgio V, Romain Q, et al. Enhancing the nonlinear optical response using multifrequency gold-nanowire antennas [J]. *Physical Review Letters*, 2012, 108(21): 217403.
- [7] Almeida J M P, Boni L D, Hernandez A C, et al. Third-order nonlinear spectra and optical limiting of lead oxifluoroborate glasses [J]. *Optics Express*, 2011, 19(18): 17220–17225.
- [8] Leonardo D B, Emerson C B, Thiago A A, et al. Femtosecond third-order nonlinear spectra of lead-germanium oxide glasses containing silver nanoparticles [J]. *Optics Express*, 2012, 20(6): 6844–6850.
- [9] Kenji I, Masahiko I, Ryo N, et al. Enhancement of ultrafast nonlinear optical response of silicon nanocrystals by boron-doping [J]. *Optics Letters*, 2012, 37(11): 1877–1879.
- [10] Poornesh P, Seetharam S, Umesh G, et al. Nonlinear optical studies on 1, 3-disubstituent chalcones doped polymer films [J]. *Optical Materials*, 2009, 31(6): 854–859.
- [11] D' silva E D, Podagatlapalli G K, Rao S V, et al. Study on third-order nonlinear optical properties of 4-methylsulfanyl chalcone derivatives using picosecond pulses [J]. *Materials Research Bulletin*, 2012, 47(11): 3552–3557.
- [12] Jia J H, Cui Y H, Han L, et al. Syntheses, third-order optical nonlinearity and DFT studies on benzoylferrocene derivatives [J]. *Dyes and Pigments*, 2014, 104: 137–145.
- [13] Kiran S M, Benoy A, Sai S S S, et al. Second- and third-order nonlinear optical properties of bis-chalcone derivatives [J]. *Journal of Photochemistry and Photobiology A: Chemistry*, 2014, 290: 38–42.
- [14] Laxminarayana K, Manjunatha K B, Seetharam S, et al. Investigation of third-order nonlinear and optical power limiting properties of terphenyl derivatives [J]. *Optics & Laser Technology*, 2014, 56: 425–429.
- [15] Davut Avci. Second and third-order nonlinear optical properties and molecular parameters of azo chromophores: Semiempirical analysis [J]. *Spectrochimica Acta Part A: Molecular and Biomolecular Spectroscopy*, 2011, 82(1): 37–43.
- [16] Wasielewski M R. Photoinduced electron transfer in supramolecular systems for artificial photosynthesis [J]. *Chemical reviews*, 1992, 92(3): 435–461.
- [17] Jia J H, Tao X M, Li Y J, et al. Synthesis and third-order optical nonlinearities of ferrocenyl Schiff base [J]. *Chemical Physics Letters*, 2011, 514(1–3): 114–118.
- [18] Wang S F, Huang W T, Zhang T Q, et al. Third-order nonlinear optical properties of didodecyldimethylammonium-Au(dmit)<sub>2</sub> [J]. *Applied physics letters*, 1999, 75(13): 1845–1847.
- [19] Jia J H, Li Y Z, Gao J R. A series of novel ferrocenyl derivatives: Schiff bases-like push-pull systems with large third-order optical responses [J]. *Dyes and Pigments*, 2017, 137: 342–351.
- [20] Zhong Q J, Zheng J, Zhang L, et al. Theoretical study on nonlinear optical properties of *N*-(6-hydroxyhexyl)-5-nitroazophenyl carbazole [J]. *Journal of Nonlinear Optical Physics & Materials*, 2018, 27(3): 1850036.
- [21] Christopher C M, Jonathan M K, Kurt W, et al. Nature of biological electron transfer [J]. *Nature*, 1992, 355(6363): 796–802.
- [22] Papagiannouli I, Iliopoulos K, Gindre D, et al. Third-order nonlinear optical response of push-pull azobenzene polymers [J]. *Chemical Physics Letters*, 2012, 554: 107–112.
- [23] Alejandro J G, Osman I O, Nuha A W, et al. A computational study of the nonlinear optical properties of carbazole derivatives: theory refines experiment [J]. *Theoretical Chemistry Accounts*

- counts, 2014, 133(4): 1458.
- [24] Kyzioł J B, Ejsmont K. 9-Methyl-3-phenyldiazenyl-9H-carbazole: X-ray and DFT-calculated structures[J]. *Acta Crystallographica Section C: Crystal Structure Communications*, 2007, 63(2): o77–o79.
- [25] Zhang L, Huang M M, Jiang Z W, et al. A carbazole-based photorefractive polyphosphazene prepared via post-azo-coupling reaction[J]. *Reactive & Functional Polymers*, 2006, 66(12): 1404–1410.
- [26] Michael E, John G, Peter G. First examples of phase transfer catalysis in electrophilic substitution reactions: acceleration of the azo coupling reaction[J]. *Journal of the Chemical Society, Chemical Communications*, 1980, (4): 181–183.
- [27] Khanzadeh M, Dehghanipour M, Karimipour M, et al. Improvement of nonlinear optical properties of graphene oxide in mixed with Ag<sub>2</sub>S@ZnS core-shells[J]. *Optical Materials*, 2017, 66: 664–670.
- [28] Ouyang Q Y, Yu H L, Zhang K, et al. Saturable absorption and the changeover from saturable absorption to reverse saturable absorption of MoS<sub>2</sub> nanoflake array films[J]. *Journal of Materials Chemistry C*, 2014, 2(31): 6319–6325.
- [29] Li F, Li X G. Theoretical investigation on nonlinear absorption of multilevel organic molecular system in ns, ps and fs regime[J]. *Optics Communications*, 2012, 285(24): 5217–5222.
- [30] Fan H L, Wang X Q, Ren Q, et al. Third-order nonlinear optical properties in [(C<sub>4</sub>H<sub>9</sub>)<sub>4</sub>]<sub>2</sub>[Cu(C<sub>3</sub>S<sub>5</sub>)<sub>2</sub>]-doped PMMA thin film using Z-scan technique in picosecond pulse[J]. *Applied Physics A*, 2010, 99(1): 279–284.
- [31] Vahid G T, Neil J B, Li B F, et al. Ultrafast all-optical chalcogenide glass photonic circuits[J]. *Optics Express*, 2007, 15(15): 9205–9221.

## *N*-(6-羟基己基)-2-甲氧基-8-硝基苯偶氮基咔唑的合成与三阶非线性光学性能

钟全洁<sup>1,2</sup>, 郑 坚<sup>2</sup>, 张 林<sup>1</sup>, 罗 炫<sup>1</sup>

(1. 中国工程物理研究院激光聚变研究中心, 四川 绵阳 621999; 2. 中国科学技术大学物理学院, 安徽 合肥 230026)

**摘要:** 通过亲电取代反应和后重氮偶合反应合成了新的化合物 *N*-(6-羟基己基)-2-甲氧基-8-硝基苯偶氮基咔唑, 用红外谱(IR)、核磁氢谱(<sup>1</sup>H NMR)以及核磁碳谱(<sup>13</sup>C NMR)对其结构进行了表征。采用密度泛函理论的B3LYP/6-31G(d)方法优化了分子结构, 在MP2/6-31G(d)的水平下进行单点能计算, *N*-(6-羟基己基)-2-甲氧基-8-硝基苯偶氮基咔唑顺反异构的相对能量  $E_r$  为 52.43 kJ·mol<sup>-1</sup>。基于纳秒时域(4 ns, 532 nm)Z-扫描技术对分子的三阶非线性光学性质进行了研究, 闭孔Z-扫描分子表现出自散焦特性, 开孔Z-扫描表明分子同时存在较强的饱和吸收和反饱和吸收。*N*-(6-羟基己基)-2-甲氧基-8-硝基苯偶氮基咔唑二阶超极化率  $\gamma$  为  $2.59 \times 10^{-29}$  esu, 品质因子达到 1.5。

**关键词:** *N*-(6-羟基己基)-2-甲氧基-8-硝基苯偶氮基咔唑; 密度泛函理论; 顺反异构; Z-扫描; 三阶非线性光学性质

中图分类号: TJ55; O649

文献标志码: A

DOI: 10.11943/CJEM2019101

(责编: 王艳秀)